A Molecular Pathway Revealing a Genetic Basis for Human Cardiac and Craniofacial Defects

Hiroyuki Yamagishi,[1]* Vidu Garg,[1]* Rumiko Matsuoka,[3] Tiffani Thomas,[1] Deepak Srivastava,[1,2]†

Microdeletions of chromosome 22q11 are the most common genetic defects associated with cardiac and craniofacial anomalies in humans. A screen for mouse genes dependent on dHAND, a transcription factor implicated in neural crest development, identified Ufd1, which maps to human 22q11 and encodes a protein involved in degradation of ubiquitinated proteins. Mouse Ufd1 was specifically expressed in most tissues affected in patients with 22q11 deletion syndrome. The human UFD1L gene was deleted in all 182 patients studied with 22q11 deletion, and a smaller deletion of approximately 20 kilobases that removed exons 1 to 3 of UFD1L was found in one individual with features typical of 22q11 deletion syndrome. These data suggest that UFD1L haploinsufficiency contributes to the congenital heart and craniofacial defects seen in 22q11 deletion.

Congenital heart defects (CHDs) are the most common of all human birth defects and are the leading cause of death in the first year of life (1). CHDs involving the outflow tract of the heart and the vessels arising from it are due to abnormal development of neural crest–derived cells that populate the heart (2, 3). The branchial arches, which give rise to craniofacial bones, the thymus, and the parathyroid glands are also populated by neural crest cells (3). Some 90% of individuals with cardiac and craniofacial defects [DiGeorge, velo-cardio-facial (VCFS), and conotruncal anomaly face syndromes (CAFS)] have monoallelic microdeletion of chromosome 22q11.2 (4).

Among heart defects, 22q11 deletions are found in 50% of patients with interruption of the aortic arch, 30% with persistent truncus arteriosus (failure of septation of aorta and pulmonary arteries), and 15% with tetralogy of Fallot (malalignment of aorta and pulmonary artery with ventricles) (5). Such cardiac defects are common after neural crest ablation in chick embryos (6), suggesting that one or more genes regulating neural crest cells may map to 22q11. A region 2.0 megabases in length is most commonly deleted and is called the DiGeorge Crit-
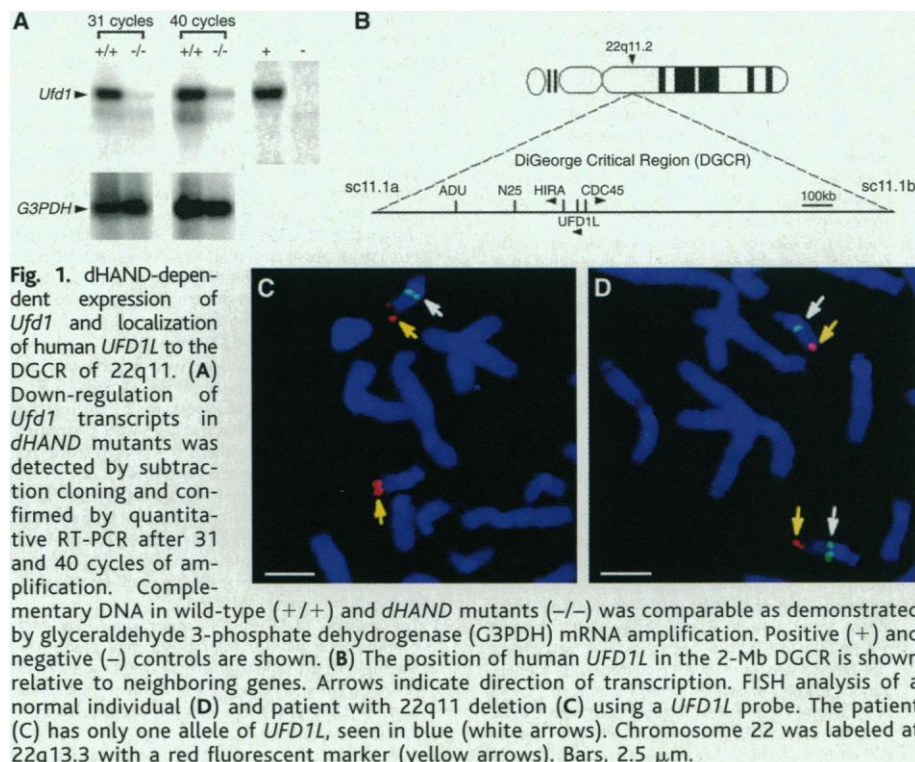
ical Region (DGCR). Extensive mapping, positional cloning, and sequencing of the human and syntenic mouse DGCR have been performed (7, 8); however, mutation analyses of candidate genes in humans and deletion studies in mice have failed to identify any genes responsible for the 22q11 deletion syndrome (7).

The basic helix-loop-helix transcription factor dHAND is required for survival of cells in the neural crest–derived branchial and aortic arch arteries and the right ventricle (9–11). Mice lacking endothelin-1 (ET-1) have cardiac and cranial neural crest defects typical of 22q11 deletion syndrome and display down-regulation of dHAND (11, 12), suggesting that a molecular pathway involving dHAND may be disrupted in this syndrome. The genes for dHAND, ET-1, or the ET-1 receptor, however, do not map to 22q11 in humans (11, 12).

To investigate the potential mechanisms through which dHAND might function, we identified dHAND-dependent genes by suppressive-subtractive hybridization (13), a procedure that yielded genes expressed in wild-type but not dHAND mutant embryos at embryonic day 9.5 (E9.5). One of the dHAND-dependent genes (Ufd1) was the mouse homolog of a yeast gene involved in degradation of ubiquitinated proteins (14). Ufd1 is essential for cell survival in yeast (14) and is highly conserved from yeast to humans (15). Quantitative reverse transcriptase–polymerase chain reaction (RT-PCR) (16) confirmed that Ufd1 was down-regulated in dHAND-null hearts at E9.5 (Fig. 1A).

This finding that Ufd1 was down-regulated in dHAND mutants was intriguing because human UFD1L is located in the DGCR (Fig. 1B) and was shown to be deleted in 13 patients with 22q11 deletion (15). To determine the frequency of UFD1L deletion, we studied 182 patients with 22q11 deletion, as detected by fluorescence in situ hybridization (FISH) (17). Our FISH analysis revealed UFD1L

Fig. 1. dHAND-dependent expression of Ufd1 and localization of human UFD1L to the DGCR of 22q11. (A) Down-regulation of Ufd1 transcripts in dHAND mutants was detected by subtraction cloning and confirmed by quantitative RT-PCR after 31 and 40 cycles of amplification. Complementary DNA in wild-type (+/+) and dHAND mutants (−/−) was comparable as demonstrated by glyceraldehyde 3-phosphate dehydrogenase (G3PDH) mRNA amplification. Positive (+) and negative (−) controls are shown. (B) The position of human UFD1L in the 2-Mb DGCR is shown relative to neighboring genes. Arrows indicate direction of transcription. FISH analysis of a normal individual (D) and patient with 22q11 deletion (C) using a UFD1L probe. The patient (C) has only one allele of UFD1L, seen in blue (white arrows). Chromosome 22 was labeled at 22q13.3 with a red fluorescent marker (yellow arrows). Bars, 2.5 μm.

Departments of [1]Pediatrics, Division of Cardiology, and [2]Molecular Biology and Oncology, University of Texas Southwestern Medical Center, 6000 Harry Hines Boulevard, Room NA8.124, Dallas, TX 75235-9148, USA. [3]Department of Pediatric Cardiology, The Heart Institute of Japan, Tokyo Women's Medical University, Tokyo, Japan.

*These authors contributed equally to this work.
†To whom correspondence should be addressed. E-mail: dsriva@mednet.swmed.edu

deletion in 182 of 182 patients (Fig. 1, C and D).

To determine if Ufd1, like dHAND, might play a role in cardiac and cranial neural crest development, we examined the embryonic expression pattern of mouse *Ufd1* (*18*). *Ufd1* was expressed in the first through fourth branchial arches, abnormalities of which are the basis of much of 22q11 deletion syndrome, with enrichment in the tips of the branchial arches, similar to dHAND expression (Fig. 2, A, B, and G). *Ufd1* expression in the palatal precursors and frontonasal region was prominent (Fig. 2, B, D, and G), an important finding because cleft palate and facial anomalies are common features of 22q11 deletion syndrome. The developing limb bud, another site of *dHAND* expression, revealed *Ufd1* expression in a pattern similar to *dHAND* at E10.5 and E12.5 (Fig. 2, D and F). *Ufd1* expression was also detected in the developing ear (otocyst) as previously reported (Fig. 2, A and F) (*15*). Within the brain, *Ufd1* was expressed with marked specificity in the medial telencephalon that forms the hippocampus (Fig. 2E). A role for Ufd1 in the hippocampus, which is involved in long-term memory, would be consistent with the learning impairment that often accompanies 22q11 deletion.

Within the heart, neural crest–derived cells are required for septation of the cardiac outflow tract into the aorta and pulmonary artery (*19*) and for remodeling of the bilaterally symmetric aortic arch arteries that form the mature aortic arch and proximal pulmonary arteries (*20*). *Ufd1* transcripts were detected in the conotruncus (cardiac outflow tract) just as neural crest cells condensed and underwent ecto-mesenchymal transformation (Fig. 2I). At E9.5 to E10.0, *Ufd1* expression was most evident in the fourth aortic arch artery (Fig. 2, B and I), which is responsible for formation of the segment of the aortic arch that lies between the left carotid and subclavian arteries (Fig. 3E). This segment does not form in interrupted aortic arch type B, one of the most common cardiac defects associated with 22q11 deletion (Fig. 3F). Vascular mesenchymal cells surrounding the proximal aorta also express *Ufd1* (Fig. 2H), similar to *dHAND*. In *dHAND*-null embryos, *Ufd1* was down-regulated in the branchial arches and conotruncus, but was detected at lower levels in the limb bud and was not affected in the developing ear (Fig. 2C). The expression of *Ufd1* in numerous tissues affected in 22q11 deletion syndrome and its involvement in a molecular pathway regulating neural crest development suggest that *Ufd1* may play a role in many features of this disease.

To determine if *UFD1L* haploinsufficiency is responsible for part of the 22q11 deletion phenotype, we searched for *UFD1L* deletions in individuals with cardiac and craniofacial defects who did not have detectable 22q11 deletions (*21*). Southern analysis of genomic DNA hybridized with a UFD1L cDNA probe revealed one individual (JF) with monoallelic deletion of exons 1 to 3 of *UFD1L* (Fig. 3, A and D), leaving exons 4 to 12 intact. Deletion of exons 1 to 3 was not detected in the parents, both phenotypically normal, suggesting that the *UFD1L* deletion in JF occurred de novo. Deletion of *UFD1L* was not detected in 100 normal unrelated individuals. As expected, expression of UFD1L mRNA in the thymus of patient JF (*22*) was diminished compared to controls without cardiac neural crest defects (Fig. 3B), confirming haploinsufficiency associated with this deletion.

The phenotype of patient JF encompassed nearly all features commonly associated with the 2-Mb 22q11 deletion. Four days after birth, she was diagnosed with interrupted aortic arch (Fig. 3F), persistent truncus arteriosus, cleft palate, small mouth, low-set ears, broad nasal bridge, neonatal hypocalcemia, T
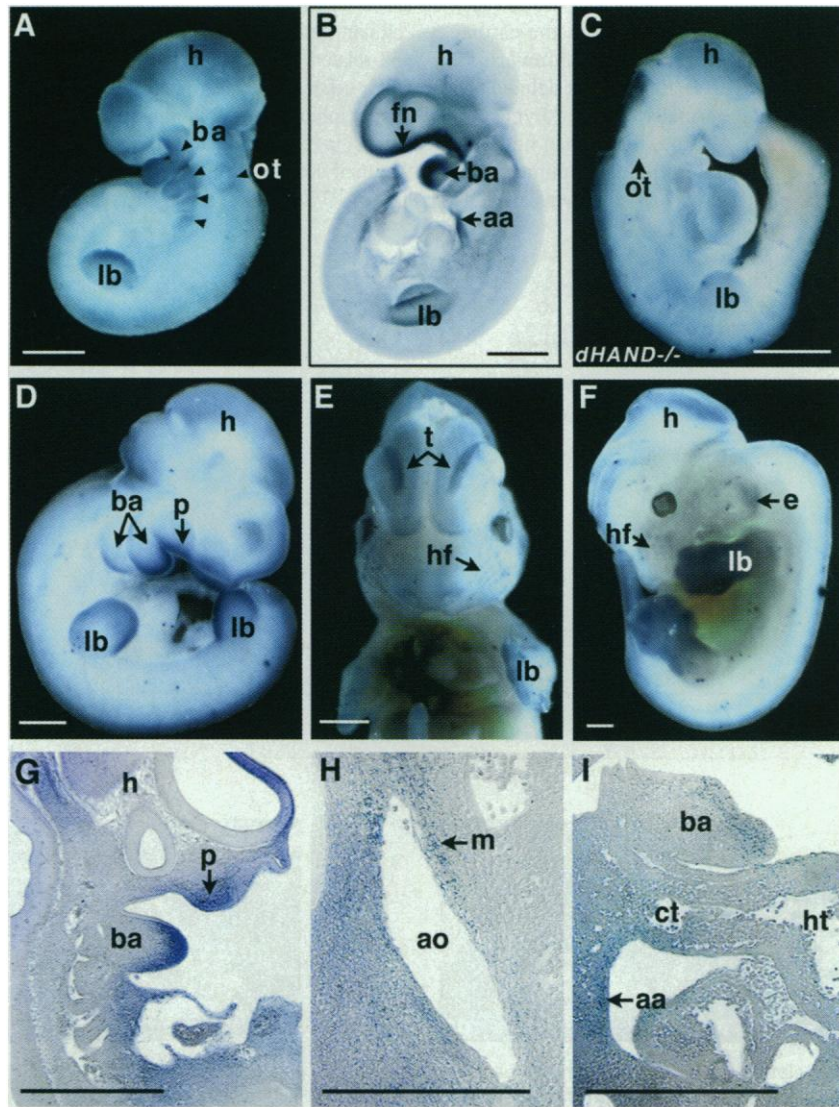
Fig. 2. Expression of *Ufd1* in mouse embryos, detected by in situ hybridization. (**A**) Expression of *Ufd1* in the branchial arches (ba), limb bud (lb), and otocyst (ot) was evident at E9.5 in a lateral view. Arrowheads mark first through fourth branchial arches. (**B**) Clearing of the embryo revealed expression of *Ufd1* in the fourth aortic arch artery (aa), the branchial arch, and fronto-nasal (fn) area. (**C**) *Ufd1* was down-regulated in the branchial and aortic arches of *dHAND* mutants, although expression was detected in the otocyst and limb bud. (**D**) At E10.5, *Ufd1* expression was seen in the branchial arches, palatal (p) precursors, and limb buds. (**E**) Frontal view of an E12.5 embryo revealed *Ufd1* transcripts in the medial telencephalon (t) and in the hair follicles (hf) of the vibrissae (whiskers). (**F**) Lateral view demonstrated expression in the developing limb and ear (e). (**G**) Histologic analysis revealed *Ufd1* in the distal mesenchyme of an E10.5 branchial arch and in the palatal mesenchyme. (**H**) Sagittal section showed expression of *Ufd1* in the mesenchyme (m) of the proximal aorta (ao). (**I**) E10.5 sagittal section through the heart revealed *Ufd1* transcripts in the conotruncus (ct), fourth aortic arch artery, and the branchial arch. Bars, 500 μm. h, head; ht, heart.

lymphocyte deficiency, and syndactyly of her toes. Although other chromosome deletions can also result in a similar phenotype (23), the genotype of JF and the *UFD1L* expression pattern suggest that *UFD1L* haploinsufficiency can contribute to many features observed in 22q11 deletion syndrome.

There is substantial variability in the phenotype associated with 22q11 deletions. Thus, it is possible that other genes in this region, distant modifier genes, or environmental factors could contribute to distinct features of 22q11 deletion syndrome. *HIRA*, the human homolog of a yeast histone regulatory gene (24), is expressed in the cardiac neural crest and maps 50 kb centromeric of *UFD1L*. However, *HIRA* was not deleted and was expressed normally in the thymus of patient JF (25). *CDC45*, the human homolog of a yeast cell cycle protein, is immediately telomeric to *UFD1L* (26) and was used to

define the 5′ breakpoint of the deletion in patient JF (21, 25) to the region between exons 5 and 6 of *Cdc45* (Fig. 3D). Although the ubiquitous nature of *Cdc45* expression (27) and its normal expression in *dHAND* mutants (Fig. 3C) (16) make it an unlikely candidate gene for the 22q11 deletion syndrome, it is conceivable that the deletion of *CDC45* may act as a modifier of patient JF's phenotype.

Our results support a role for ubiquitin-mediated mechanisms in controlling neural crest development. Ubiquitin-specific proteases are essential for regulating numerous critical cellular pathways, including those involving p53-related cell survival and NF-κB (nuclear factor–κB) activity (28). In vitro overexpression or inhibition of ubiquitin-specific proteases results in programmed cell death, indicating that their activity is dose-dependent (29). Yeast lacking *Ufd1* exhibit a cell survival defect that

is incompletely rescued by one allele of *Ufd1* (14), consistent with the notion that haploinsufficiency of *UFD1L* may contribute to the phenotype seen in 22q11 deletion syndrome. We speculate that *UFD1L* haploinsufficiency leads to accumulation of certain proteins and defective survival of cardiac and cranial neural crest cells, resulting in premature thymic apoptosis and loss of cells that contribute to the transverse aortic arch, palate, and craniofacial structures. Further mutation analysis of *UFD1L* in humans and elucidation of the cellular pathways regulated by UFD1L may provide new directions in understanding basic mechanisms of neural crest development and congenital cardiac and craniofacial defects.

Fig. 3. Deletion of *UFD1L* and clinical features of patient JF.

References and Notes
1. J. I. E. Hoffman, *Pediatr. Cardiol.* **16**, 103 (1995).
2. D. C. Fyler, in *Nadas' Pediatric Cardiology, Trends*, A. S. Nadas and D. C. Fyler, Eds. (Hanley & Belfus, Philadelphia, 1992), pp. 273–280; L. H. S. Van Mierop and L. M. Kutsche, *Am. J. Cardiol.* **56**, 133 (1986).
3. M. L. Kirby, *Trends Cardiovasc. Med.* **3**, 18 (1993).

GCTTTCTGCTGCCTTCT-3') under the following conditions: 94°C for 5 min; 94°C for 1 min, 52°C for 1 min, and 72°C for 1 min; and 72°C for 7 min. PCR products were analyzed by agarose gel electrophoresis after serial cycles in the linear range of amplification. RNA loading was controlled for by amplification of the housekeeping gene, glyceraldehyde 3-phosphate dehydrogenase (G3PDH). Negative controls were performed for each sample using non-reverse-transcribed RNA. A Southern blot of the samples was hybridized for UFD1L or G3PDH.

17. Human metaphase chromosome slides were prepared from Epstein-Barr virus–transformed lymphoblastoid cell lines or peripheral blood. Slides were hybridized with a genomic clone encompassing UFD1L that had been obtained by screening a human P1 artificial chromosome library with UFD1L-specific primers. FISH analysis was performed according to R. Matsuoka et al. [Hum. Genet. 103, 70 (1998)]. Patients with 22q11 deletion had been characterized by FISH using the N25 (Oncor) marker that does not encompass UFD1L.

18. Whole-mount in situ hybridizations were performed with digoxygenin-labeled antisense riboprobes synthesized from the 700-bp open reading frame and the 250-bp 3' untranslated region of mouse UFD1L cDNA (9). Embryos were photographed with and without clearing in benzyl benzoate:methyl salicylate (1:1). For histologic analysis, stained embryos were embedded in paraffin after fixation. Transverse and sagittal sections were made at 8-µm intervals throughout the embryos.

19. M. L. Kirby, T. F. Gale, D. E. Stewart, Science 220, 1059 (1983).

20. E. N. Olson and D. Srivastava, ibid. 272, 1069 (1996); M. L. Kirby and K. L. Waldo, Circ. Res. 77, 211 (1995).

21. A research protocol for human studies was approved by the Institutional Review Board of the University of Texas Southwestern Medical Center. Informed consent was obtained from the parents for collection of blood and thymic tissue. Genomic DNA was obtained from 10 individuals at Children's Hospital, Medical Center of Dallas, with normal karyotype and negative FISH for 22q11 deletion, who had cardiac or craniofacial defects, or both, typical of 22q11 deletion; DNA from 100 control individuals with normal karyotype was also obtained. Genomic DNA extracted from human blood or thymic tissue (QIAamp blood kit, QIAGEN) was digested with Eco RI or Hind III, transferred to nylon membranes, and hybridized to 32P-labeled UFD1L or CDC45 cDNA.

22. Thymic tissue was collected from patients who were undergoing surgical repair of CHD, and total RNA was extracted and used for cDNA synthesis. Northern analysis was performed on 20 µg of total thymic RNA and hybridized to a UFD1L cDNA probe. HIRA- and CDC45-specific amplimers were used to amplify the respective cDNAs. HIRA amplimers were: upper, 5'-GACGGCTCTGTGGCATTCCT-3'; lower, 5'-GCCA-TCTGCTGTCCGAGTCT-3'. CDC45 amplimers were: upper, 5'-GCCTTGTTCCAGTGTGACCA-3'; lower, 5'-GTTCTCCTCATCCTCGTTCC-3'.

23. S. C. Daw et al., Nature Genet. 13, 458 (1996).

24. L. G. Wilming et al., Hum. Mol. Genet. 6, 247 (1997); P. Magnaghi et al., Nature Genet. 20, 74 (1998).

25. H. Yamagishi, V. Garg, D. Srivastava, unpublished observations.

26. J. McKie et al., Genome Res. 8, 834 (1998).

27. T. H. Shaikh et al., Am. J. Hum. Genet. 63, A193 (1998).

28. M. Scheffner, J. M. Huibregtse, R. D. Vierstra, P. M. Howley, Cell 75, 495 (1993); C. Sears, J. Olesen, D. Rubin, D. Finley, T. Maniatis, J. Biol. Chem. 273, 1409 (1998).

29. L. Monney et al., J. Biol. Chem. 273, 6121 (1998).

30. We thank R. Schultz and A. Bowcock for helpful discussions and assistance with genetic analyses, members of the pediatric cardiology and cardiothoracic surgery divisions for assistance with tissue collection, other members of the Srivastava laboratory for critical discussion, J. L. Goldstein, M. S. Brown, E. N. Olson, and H. H. Hobbs for critical review of this manuscript, and J. Page for manuscript preparation. Supported by grants to D.S. from NIH (R01HL57181-01) and March of Dimes.

2 November 1998; accepted 19 January 1999

Regulation of Chamber-Specific Gene Expression in the Developing Heart by Irx4

Zheng-Zheng Bao,[1] Benoit G. Bruneau,[1] J. G. Seidman,[1] Christine E. Seidman,[2] Constance L. Cepko[1]*

The vertebrate heart consists of two types of chambers, the atria and the ventricles, which differ in their contractile and electrophysiological properties. Little is known of the molecular mechanisms by which these chambers are specified during embryogenesis. Here a chicken iroquois-related homeobox gene, Irx4, was identified that has a ventricle-restricted expression pattern at all stages of heart development. Irx4 protein was shown to regulate the chamber-specific expression of myosin isoforms by activating the expression of the ventricle myosin heavy chain–1 (VMHC1) and suppressing the expression of the atrial myosin heavy chain–1 (AMHC1) in the ventricles. Thus, Irx4 may play a critical role in establishing chamber-specific gene expression in the developing heart.

During embryonic development, the ventricles and atria of the heart arise from a single tubular structure (1, 2). Mature atria and ventricles differ in their contractile and electrophysiological characteristics and express distinct sets of genes (3, 4). Most of the known chamber-specific genes encode isoforms of contractile proteins, including the myosin heavy chains and light chains (4). The correct expression of these myosin isoforms is essen-

tial for embryonic survival and proper function of the mature heart (5). The mechanisms involved in regulation of these chamber-specific patterns in the developing heart tube are unknown. Here we show that in chick hearts, this process requires the proper regulation of the iroquois-related homeobox gene Irx4.

The Irx4 gene was identified by a low-stringency hybridization screening of a chick embryonic day 6 to 8 (E6–E8) retinal cDNA library, with probes derived from mouse and human EST clones that span the Iroquois homeodomains (6). The predicted open reading frame contains a homeodomain highly homologous to those in the Drosophila Iroquois proteins (7, 8), and it is most closely related to the human IRX4 (83% amino acid identity overall and 70% amino acid identity

outside of the homeodomain) (Fig. 1, and supplementary data available at www.sciencemag.org/feature/data/985642.shl). We have also identified a mouse IRX4 with 71% overall amino acid homology to chick Irx4 (9).

By in situ hybridization (10), we detected Irx4 expression in the retina, a subset of nuclei in the hindbrain, the developing feather buds, and the heart (Fig. 1, B to D) (11). Irx4 was highly expressed in the ventricular myocardium, but expression was absent from the atria or the distal outflow tract in the developing heart. Low levels of expression were observed in the proximal outflow tract. The ventricle-specific expression pattern was observed as early as stage 10 in the prospective ventricular region and persisted in all developmental stages examined (Fig. 1, B to D, and Fig. 2). The expression of the mouse Irx4 gene was similarly restricted to the ventricles in all stages of developing heart and adult heart (9).

We next compared Irx4 with other genes known to have a chamber-restricted expression pattern in the developing chick heart. Irx4 expression was first observed at Hamburger-Hamilton (HH) stage 10, when the developing heart is a linear tube. At stage 10, Irx4 expression was already restricted to the middle portion of the heart tube, which corresponds to the prospective ventricles (Fig. 2B). The ventricle-restricted pattern persisted to later stages (Fig. 2, E and H). In contrast to Irx4, ventricle myosin heavy chain–1 (VMHC1) gene expression was detected earlier and in regions of the heart tube destined to become both atria and ventricles (Fig. 2, A and D) (12). As with VMHC1, early atrial myosin heavy chain–1 (AMHC1) gene expression also was not restricted (Fig.

[1]Howard Hughes Medical Institute and Department of Genetics, Harvard Medical School, 200 Longwood Avenue, Boston, MA 02115, USA. [2]Howard Hughes Medical Institute and Cardiovascular Division, Brigham and Women's Hospital, Boston, MA 02115, USA.

*To whom correspondence should be addressed. E-mail: cepko@rascal.med.harvard.edu